JPhys Materials

PURPOSE-LED PUBLISHING™

TOPICAL REVIEW • OPEN ACCESS

Recent advances in conducting polymer chemiresistive sensors for ammonia gas detection: materials, characterization, and applications

To cite this article: Annelot Nijkoops *et al* 2026 *J. Phys. Mater.* **9** 012002

Journal of Physics: Materials

OPEN ACCESS

RECEIVED
4 April 2025

REVISED
24 July 2025

ACCEPTED FOR PUBLICATION
6 November 2025

PUBLISHED
19 December 2025

TOPICAL REVIEW

Recent advances in conducting polymer chemiresistive sensors for ammonia gas detection: materials, characterization, and applications

Annelot Nijkoops[1,2,3,4,*], Manuela Ciocca[1,2], Martina Aurora Costa Angeli[1], Mukhtar Ahmad[1], Remko Boom[4], Niko Münzenrieder[1,2], Paolo Lugli[1,2] and Luisa Petti[1,*]

[1] Faculty of Engineering, Free University of Bozen-Bolzano, Bozen-Bolzano 39100, Italy
[2] Competence Centre for Mountain Innovation Ecosystems, Bozen-Bolzano 39100, Italy
[3] Faculty of Agricultural, Environmental and Food Sciences, Free University of Bozen-Bolzano, Bozen-Bolzano 39100, Italy
[4] Laboratory of Food Process Engineering, Wageningen University and Research, 6700 AA Wageningen, The Netherlands
[*] Authors to whom any correspondence should be addressed.

E-mail: annelot.nijkoops@wur.nl and luisa.petti@unibz.it

Keywords: conductive polymers, PEDOT, P3HT, PANI, PPy, chemiresistive sensors, ammonia NH3 gas sensors

Abstract

Conducting polymers (CPs) are highly susceptible to ammonia (NH_3) at room temperature. This has spurred growing interest in CP-based NH_3 gas sensors across diverse fields, ranging from biomedicine to environmental monitoring. Detecting NH_3 levels in breath, from parts per million to parts per billion, aids in diagnosing health conditions like liver and kidney dysfunction. Despite the importance of CP-based NH_3 sensors, a comprehensive assessment of their performance, limitations, and prospects has yet to be conducted. To address this gap, this work provides a detailed review of chemiresistive NH_3 sensors based on CPs (including P3HT, PEDOT, PPy, and PANI), examining sensor response, selectivity, stability, repeatability, and sensitivity to environmental factors like humidity and temperature. The role of porous structures and gas diffusion mechanisms in enhancing CP sensor performance is emphasized, alongside CP-based composite materials. The mechanical flexibility of these sensors is analyzed and compared, highlighting their potential for integration into flexible and wearable devices. Key challenges for CP-based NH_3 sensors include poor selectivity due to interference from similar gases, sensitivity loss caused by humidity-induced CP swelling, and instability from temperature fluctuations. Additionally, the lack of standardized testing protocols complicates performance comparisons of CP-based NH_3 sensors. Future research should focus on improving CP porosity, understanding gas-CP interactions, developing stable composites, and exploring new CPs for improved NH_3 sensing.

1. Introduction

In the late 1970s, the collaborative efforts of Hideki Shirakawa, Alan G MacDiarmid, and Alan J Heeger resulted in the successful and groundbreaking synthesis of the world's first conducting polymer (CP), namely polyacetylene (PA) [1, 2]. In figure 1(a), the molecular structure of PA is depicted visualizing the presence of alternating single and double bonds [3, 4]. This remarkable discovery revolutionized the field of material science and paved the way to a completely new field of research, which was ultimately recognized by the Nobel Prize in the year 2000 [1, 2]. As the first CP, PA has gained interest in fluorescence sensors [5, 6] and humidity sensors [7, 8]. The major drawbacks associated to PA, its insolubility in common organic solvents and instability when exposed to air, led to the acceleration of research activities to identify alternative CPs [9, 10]. As a result, numerous CPs were found: e.g. poly(3,4-ethylene dioxythiophene)(PEDOT), polypyrrole (PPy), poly(phenylene) (PPP), polyaniline (PANI), polythiophene (PTh), and their derivatives (e.g. poly(3-alkylthiophenes) (P3ATs), poly(3-hexylthiophene) (P3HT)) [11]. The molecular structures of some of the most common CPs are shown in figure 1(b) [11, 12].

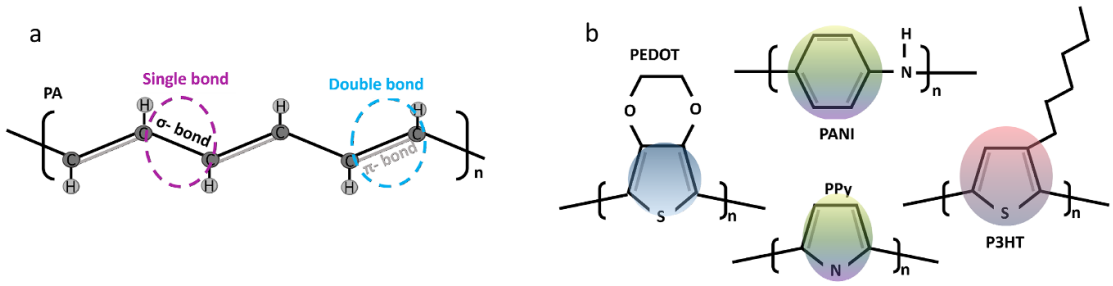

Figure 1. (a) Alternating single and double bonds in conducting polymer molecular backbone of polyacetylene (PA). (b) Molecular structure of several common conducting polymers (PEDOT, PANI, PPy and P3HT).

Compared to traditional gas sensing materials like metal oxides, which require high operating temperatures, organic CPs offer the significant advantage of superior sensing response to gases at room temperature [13]. CPs have excellent electrical, mechanical and optical properties and can be utilized as active materials for the resistive detection of gases [14, 15]. The ease of processing and fabricating of CPs make these materials outstanding candidates for use in gas sensors [16]. Several review papers explored the use of CPs in gas sensors [13, 15, 17]; however, to the best of our knowledge, none specifically focused on ammonia (NH_3) gas sensors.

NH_3 is emitted into the atmosphere via manure from livestock and wildlife, biomass burning, or fertilizers contributing to the global nitrogen cycle [18–20]. Furthermore, NH_3 is created by the human body by metabolizing amino acids and other nitrogen containing compounds, and may be an indicator of several diseases [21, 22]. As demonstrated in our previous work, we presented a comprehensive discussion on the diverse applications of NH_3 gas sensing [23]. High NH_3 levels in a person's breath, for example, can be due to liver or kidney diseases, or gastric *Helicobacter pylori* bacteria infections [24].

This work aims to bridge the gap by offering a comprehensive evaluation of CP-based NH_3 gas sensors, with a particular focus on chemiresistive sensing mechanisms. Our review provides an analysis of the factors influencing sensor performance, including sensitivity, selectivity, and stability. It also examines how material modifications contribute to improving sensor performance. By comparing various CPs and their functionalization techniques, this study offers guidance to researchers in selecting and designing CPs for NH_3 gas sensing applications. The review also touches on emerging trends and challenges, aiming to contribute to the ongoing development in this field. The structure of this review is outlined as follows: firstly, gas sensor technologies and CPs (section 2) are discussed, with (section 2.1) covering sensor technologies and materials, and (section 2.2) exploring the electrical properties of CPs in detail. Secondly, the characteristics of CP-based chemiresistive gas sensors are analyzed by comparing a selection of chemiresistive CP ammonia gas sensors, chosen to represent the current state of the art based on available and relevant studies (table 1) (section 3) and covering aspects such as the pristine polymer response (section 3.1), selectivity (section 3.2), stability (section 3.3), repeatability (section 3.4), humidity (section 3.5) and temperature (section 3.6) as well as their mechanical stability (section 3.7). Finally, discussion, future prospects, and a conclusion, are provided in sections 4–6 respectively.

2. Gas sensor technologies and CPs

2.1. Sensor technologies and materials

The rapid detection and quantification of gases such as ammonia (NH_3), methane (CH_4), sulfur oxides (SO_x), carbon oxides (CO_x), and nitrogen oxides (NO_x) is critical for preventing environmental pollution, ensuring public safety, and mitigating health risks [25]. Gas concentrations, often measured in parts per million (ppm) or parts per billion (ppb), are essential for monitoring air quality and for medical applications, such as analyzing patient breath to diagnose underlying diseases [26, 27].

A variety of gas sensing technologies is available, including optical, electrochemical, and chemiresistive sensors [28]. Optical sensors detect gas species based on their absorption or emission at specific wavelengths across spectral regions such as ultraviolet, visible, near-infrared, and mid-infrared [29]. A main advantage of optical gas sensors is their high specificity, achieved by using distinct wavelengths of light to detect the characteristic optical properties of target gases. This ensures minimal cross-response to other gases [29]. However, the primary drawback is the need for specialized, high-cost equipment, which makes optical sensors bulky and unsuitable for portable or low-cost applications [30, 31].

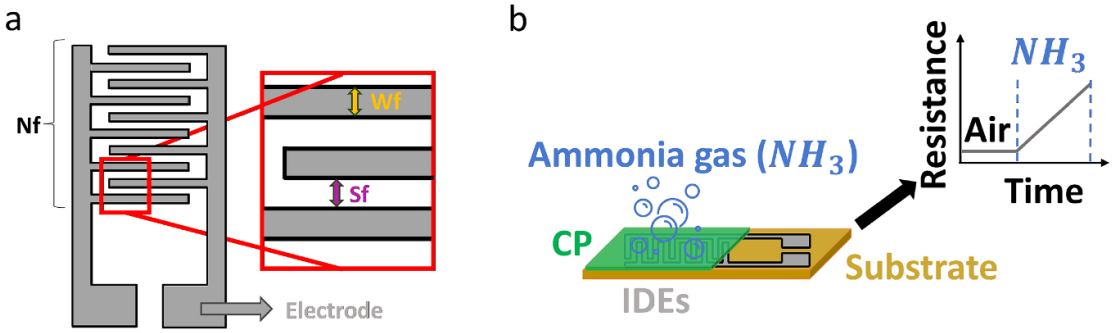

Figure 2. (a) Interdigitated electrodes structures (IDEs). (b) Resistance change of interdigitated electrodes with a conducting polymer active sensing layer when exposed to ammonia gas (NH_3).

Electrochemical sensors, typically consisting of a counter electrode, a working electrode, and a reference electrode, use electrochemical reactions within a sealed cell to generate a measurable current upon gas exposure [32]. In contrast to optical sensors, electrochemical gas sensors can be miniaturized, making them ideal for wearable devices [33]. They also offer linear, proportional response and can be tailored to detect specific gases [34]. However, their major disadvantage lies in their limited shelf life, typically ranging from six months to a year [34]. Additionally, electrochemical sensors are relatively complex to fabricate, requiring high-precision manufacturing and costly materials, such as specialized membranes and expensive electrodes [35, 36].

Chemiresistive sensors detect changes in the resistance of a material when exposed to different gases, offering a simpler and often more cost-effective solution [37]. Chemiresistive gas sensors are easily miniaturized, with a simple sensing mechanism that is compatible with low-cost readout circuitry, making them a more cost-effective option compared to electrochemical sensors [35, 38]. Chemiresistive sensors are therefore a promising technology for NH_3 gas sensing in applications such as environmental monitoring, industrial safety, and biomedical diagnostics (e.g. air quality assessment, gas leak detection, and breath analysis).

Each technology presents unique advantages and limitations, with the optimal choice dependent on the specific requirements of the application [39, 40]. Furthermore, the choice of active sensing materials (e.g. graphene [41], carbon nanostructures (e.g. carbon nanotubes (CNTs)) [42], semiconducting metal oxides (SMOXs) [43], and CPs) offer distinct advantages and limitations in terms of sensitivity, selectivity, response time, and stability. Their sensing mechanisms typically involve changes in electrical resistance due to gas interactions [44]. While SMOX sensors require high operating temperatures, CPs and carbon-based materials function at lower temperature [45]. For medical applications, biocompatibility is a crucial requirement and the potential cytotoxicity of CNTs raise concerns regarding their safe implementation [46]. Therefore, CPs are favorable alternatives.

The standard chemiresistive gas sensing device configuration consists of an active layer deposited between two electrodes [47]. Interdigitated electrodes (IDEs), depicted in figure 2(a), with a geometry that can be varied in terms of number of fingers (N_f), spacing between fingers (S_f), and finger width (W_f), are widely used in chemiresistive sensors [48]. Their design primarily enables higher measurable resistance while also enhancing sensitivity, providing efficient current pathways, ensuring a uniform electric field, and allowing for scalable and cost-effective fabrication [49, 50]. The active sensing layer is deposited either below or on top of the two electrodes, and when exposed to an analyte, the resistance of the material changes [51].

Traditionally, inorganic materials like metal oxides such as, zinc oxide (ZnO), tungsten oxide (WO_3), titanium oxide (TiO_2), and tin oxide (SnO_2) are selected as active sensing layer due to their reliability [51]. Unfortunately, metal oxides require operating temperatures between 100 °C and 450 °C to enhance their sensing performance as they have nearly no sensitivity at room temperature [15, 52]. This results in a high power consumption, and the need for external heating elements (a heater or a furnace) or approaches such as self-heating when utilizing metal oxides as active layer [53].

One gaseous compound of immense interest is NH_3 gas, which can be measured with chemiresistive NH_3 sensors developed for applications including environmental, medical, automotive emissions and air quality monitoring [54–58]. The typical change in resistance when a CPs sensing layer is exposed to NH_3 is depicted in figure 2(b) [44]. The change in resistance depends on the type of gas interacting with the sensing layer material (which induces a resistance variation). For reducing gases, the resistance of an

n-type material decreases whereas the resistance of a p-type material increases. In contrast, for oxidizing materials the resistance of an n-type material increases, whereas the resistance of a p-type material decreases [59].

2.2. Electrical conductivity of CPs

For a CP to exhibit electrical conductivity, it must have a high degree of conjugation which is characterized by alternating single and double bonds and enable the overlap of π molecular orbitals. This structural feature allows for electron delocalization and facilitates charge transport throughout the polymer chain [4]. When exposed to dopant agents, either oxidizing or reducing, these polymers can generate mobile charge carriers, thereby significantly enhancing their conductivity and transitioning them from an insulating to a metallic (highly conductive) state [60]. Doping also alters the intrinsic electronic structure of the polymer, resulting in a reduction in the effective bandgap, which allows for easier excitation of electrons, thereby improving conductivity [61].

The addition of a dopant to a CP promotes a redox reaction, either adding electrons (for n-type) or removing electrons (for p-type), which transforms the CP into n-type or p-type material, respectively [16, 62, 63]. During the redox reaction, oxidation (loss of electrons) or reduction (gain of electrons) modifies the electronic structure and properties of the CP [62, 63].

When CPs interact with gases, the electronic balance gets disturbed, resulting in measurable changes (e.g. current, resistance, or potential) [64]. The exposure of p-type CPs (e.g. PPy, P3HT, PEDOT) to NH_3 leads to a dedoping effect, causing a reduction in the concentration of holes [65–68]. PPy specifically undergoes the following physical adsorption (equation (1)) and desorption (equation (2)) reactions [15, 69],

$$PPy^{+} + \ddot{N}H_3 \rightarrow PPy^{0} + {NH_3}^{+} \tag{1}$$

$$PPy^{0} + {NH_3}^{+} \rightarrow PPy^{+} + NH_3 \tag{2}$$

PANI at the same time can be present in one of three oxidation states: leucoemeraldine (reduced state), emeraldine (partly oxidized/reduced) and pernigraniline (oxidized state) [16]. The emeraldine form can be further classified as emeraldine salt (ES) or emeraldine base (EB) representing protonated and unprotonated forms, respectively [70]. The doped state of PANI, i.e. its conducting ES form, can be deprotonated when exposed to NH_3 to its neutral EB form via the formation of an ammonium cation (equation (3)) [67, 71, 72],

$$PANI - H^{+} + NH_3 \rightarrow PANI + {NH_4}^{+}. \tag{3}$$

When the acidic form of PANI is exposed to NH_3 gas, deprotonation occurs resulting in dedoping into its EB form and the formation of ammonium ions due to the transfer of NH-groups [15, 73]. Figure 3(a) visualizes the adsorption of NH_3 on PPy [15] while figure 3(b) depicts the acid/base reaction of NH_3 with PANI [74, 75].

Doping and dedoping processes alter the electronic properties of CPs by affecting the position of the highest occupied molecular orbital (HOMO) and lowest unoccupied molecular orbital (LUMO) [76]. The position of the HOMO and LUMO are important to determine the band gap of CPs [76]. The energy gap (E_g) between the HOMO and the LUMO determines the conductivity of the CPs, leading to metallic ($E_g = 0$), semiconductive ($E_g \approx 0.1 - 3.0\,eV$) or insulating ($E_g \geqslant\approx 3.0\,eV$) characteristics (figure 4(a)) [3, 77, 78]. Doping introduces or removes charge carriers (electrons or holes), modifies the density of states by creating or eliminating energy levels within the material, and influences the material's electrical conductivity [79, 80]. For instance, undoped pristine polymers behave as insulators or semiconductors in their undoped states, but when the dopant concentrations are increased, conductivity develops [16, 81]. The energy levels of PANI, PPy, PEDOT:PSS and P3HT are depicted in figure 4(b) (It should be noted that these values are reported in the literature and shown as representative examples for pristine polymers; the absolute energy levels may vary depending on polymer characteristics and processing conditions.) [82–85].

The solubility and ease of processing of CPs are primarily influenced by the structure of their side chains, while the incorporation of dopant ions plays a key role in defining their mechanical, electrical, and optical properties [16]. Hierarchical ordering of the CP chains is important for electron or hole transport resulting in high electronic conductivity [86]. The polymer arrangement can consist of

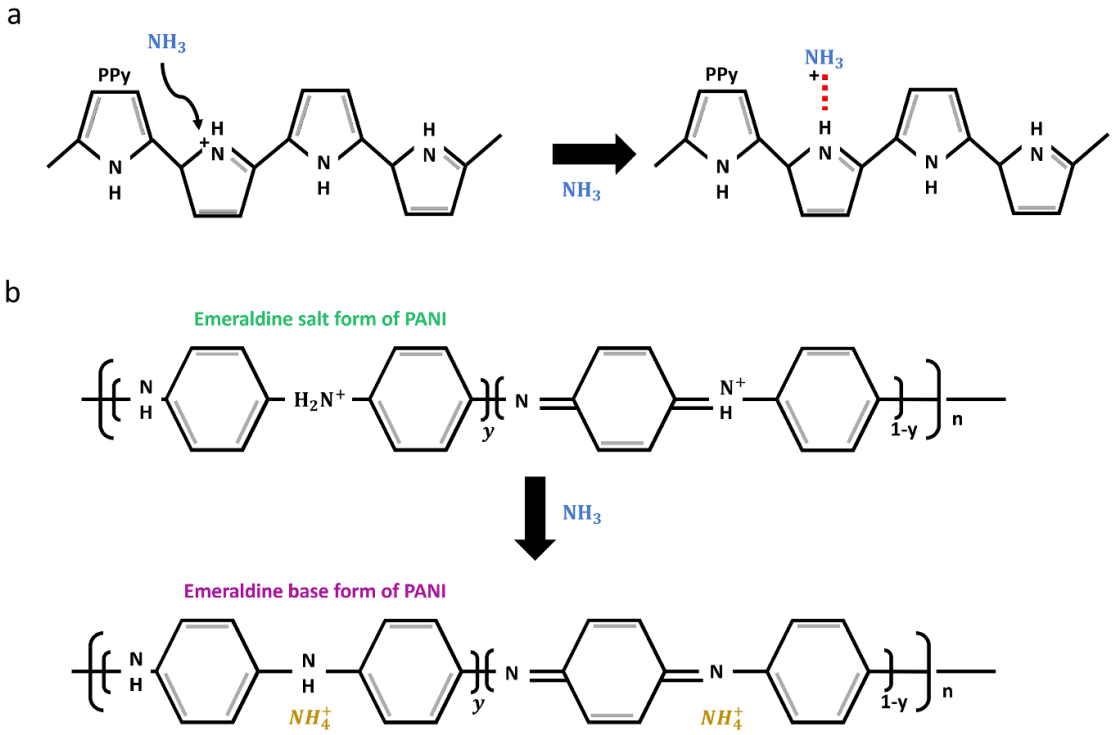

Figure 3. (a) PPy NH_3 adsorption. (b) PANI acid/base reaction with NH_3.

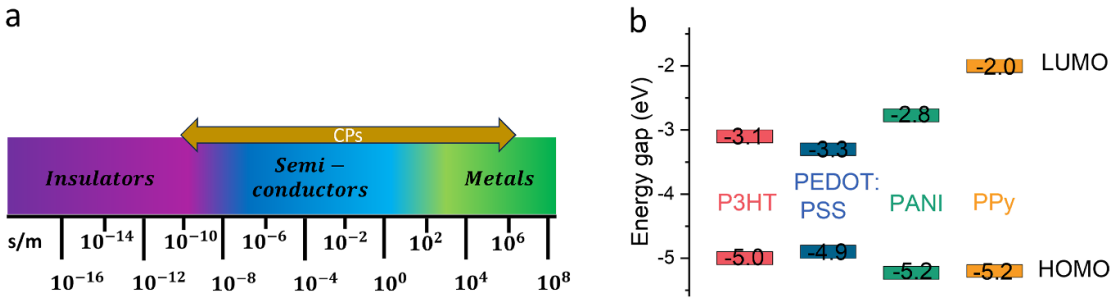

Figure 4. (a) Electrical conductivity of conducting polymers. (b) Energy level diagram of PANI, PPy, PEDOT:PSS and P3HT.

Figure 5. Randomly distributed amorphous, semi-crystalline and highly-order crystalline arrangement of conducting polymers.

amorphous, semi-crystalline and crystalline regions when in a solid state and influence the charge transport properties (figure 5) [87]. Amorphous regions are characterized by randomly coiled structures with weak inter-chain interactions while crystalline regions are 1-dimensional highly organized self-assembled nano-structures [88–90]. In the crystalline regions, free charge carriers can easily move along the conjugated chains [91]. Furthermore, the preferential orientation of the π-stacking orientations (edge-on (perpendicular π–π stacking compared to the substrate) and face-on (parallel π–π stacking compared to the substrate)) of crystalline arrangements can further affect the charge transport [92, 93]. Charge transportation is more favorable in the edge-on orientation compared to face-on orientation [94].

3. CP-based chemiresistive gas sensors

In this section, we analyze chemiresistive sensors employing CPs (PEDOT, PPy, P3HT, or PANI) as sensing materials. These sensors are detailed in table 1, highlighting key parameters including the detection limit, response and recovery times, sensitivity, humidity sensitivity, and substrate material. The selected papers are thoroughly examined to discuss and compare the pristine polymer responses, selectivity, stability, repeatability, as well as the influence of humidity and temperature. Additionally, we assess the bending characteristics of CP sensors based on the findings from these studies.

3.1. Pristine CP response

In this subsection, the response of polymers towards NH_3 is reported. The cited works report the response of CPs to NH_3 in concentration of 0.2–50 ppm being in the range of 2%–77% calculated as

$$\text{Response}_{(\%)} = \left(R_g - R_a\right)/R_a \times 100 \tag{4}$$

where R_g is the sensor's resistance when the analyte gas (NH_3) is present, while R_a is the initial resistance (in air) [95]. Li *et al* [96] reported that the response value of PPy towards 10 ppm NH_3 is 2.7%. Qiu *et al* [97] observed ≈2% towards 10 ppm NH_3 for PEDOT:PSS. Furthermore, Lv *et al* [98] found that the resistance of PEDOT:PSS after exposure to 50 ppm NH_3 could not return to its baseline while the initial resistance increased from 3.6 kΩ to 4.1 kΩ indicating a drift. At the same time, good recovery values where obtained when adding ferric chloride ($FeCl_3$) which is presented in figure 6(a).

As demonstrated in our previous work [95], pristine P3HT after exposure to 5 ppm does not recover to the baseline and has an upward resistance drift which even reached cut off values of 50 MΩ during measurements, even though it shows a relatively high response value of 76.96% when exposed to 50 ppm NH_3. Adding single-walled CNTs (SWCNTs) to P3HT results in improved recovery to the baseline when NH_3 exposure is stopped and still allows good sensitivity values of 11.22% and 57.82% at 5 ppm and 50 ppm NH_3, respectively (figure 6(b)).

Zhang *et al* [99] investigated PANI sensor and recorded a response and recovery time of 134 s and 290 s respectively, while addition of $SrGe_4O_9$ nanowires to PANI responded in 62 s and 223 s for a 0.2 ppm NH_3 exposure. Wang *et al* [100] found a response and recovery of 246 s/400 s for PANI. When MXene NB_2CT_x was added to PANI the values improved to 218 s/300 s when exposed to 10 ppm NH_3. Wu *et al* [101] found that graphene (GP)-PANI sensors had response/recovery times of 46 s/198 s (PANI 150/300 s). Zhang *et al* [102] reported that PANI/multi-walled CNTs (MWCNTs)/molybdenum disulfide (MoS_2) sensors gave a response value of 11% with a response and recovery time of 32 s/36 s to 0.25 ppm NH_3 (pristine PANI obtained 0.92%, 104 s/56 s). Eventhough the response and recovery times of pristine PANI slightly differ between each paper, the values are comparable.

It can be concluded that pristine CP sensing towards NH_3 faces many challenges such as low response values [96, 97, 102], long response and recovery times [99, 100, 102], and poor recovery [95, 98] to the baseline after gas exposure is stopped. However, the addition of compounds to pristine CPs can improve the sensor response value and response/recovery times significantly.

There are several primary mechanisms discussed in the cited papers that explain the enhancement in sensor performance due to additives. These mechanisms include the introduction of a porous architecture, the incorporation of nanofibers, nanoparticles, or hollow tubular structures, all of which contribute to an increased surface area. These features can also reduce response time by facilitating faster analyte diffusion and more efficient electron transport. Furthermore, some studies created p–n junctions by combining the p-type CP with n-type materials such as wide-bandgap $SrGe_4O_9$ [99], Nb_2CTx [100], N-MXene Ti_3C_2Tx [97], graphene [101], MoS_2 [102], SnO_2 [103], and ZnO [96, 104]. Hydrophilic groups (–OH) can enhance reactions with NH_3 and generate electrons. Certain additives, such as CTAB and HNTs, help prevent the agglomeration and exfoliation of CP by regulating its morphology, leading to a more uniform distribution. Materials like MWCNTs, MoS_2, or core–shell Au@SiO_2 nanocrystals can enhance conductivity.

3.2. Selectivity of CP-based composites

Molecules with similar chemical characteristics as the target gas can influence the target gas sensing measurement, therefore it is of importance that the sensor exhibits a good selectivity, i.e. it responds only to the target gas [105]. For this section only PANI and PEDOT:PSS based sensors where selected from the listed sensors (table 1) as those papers reported data on the selectivity.

The PSS-PANI/polyvinylidene difluoride (PVDF) sensor developed by Lv *et al* [106] showed selectivity towards NH_3 with response values of around 70% for 1 ppm, here a response of less than 10% was

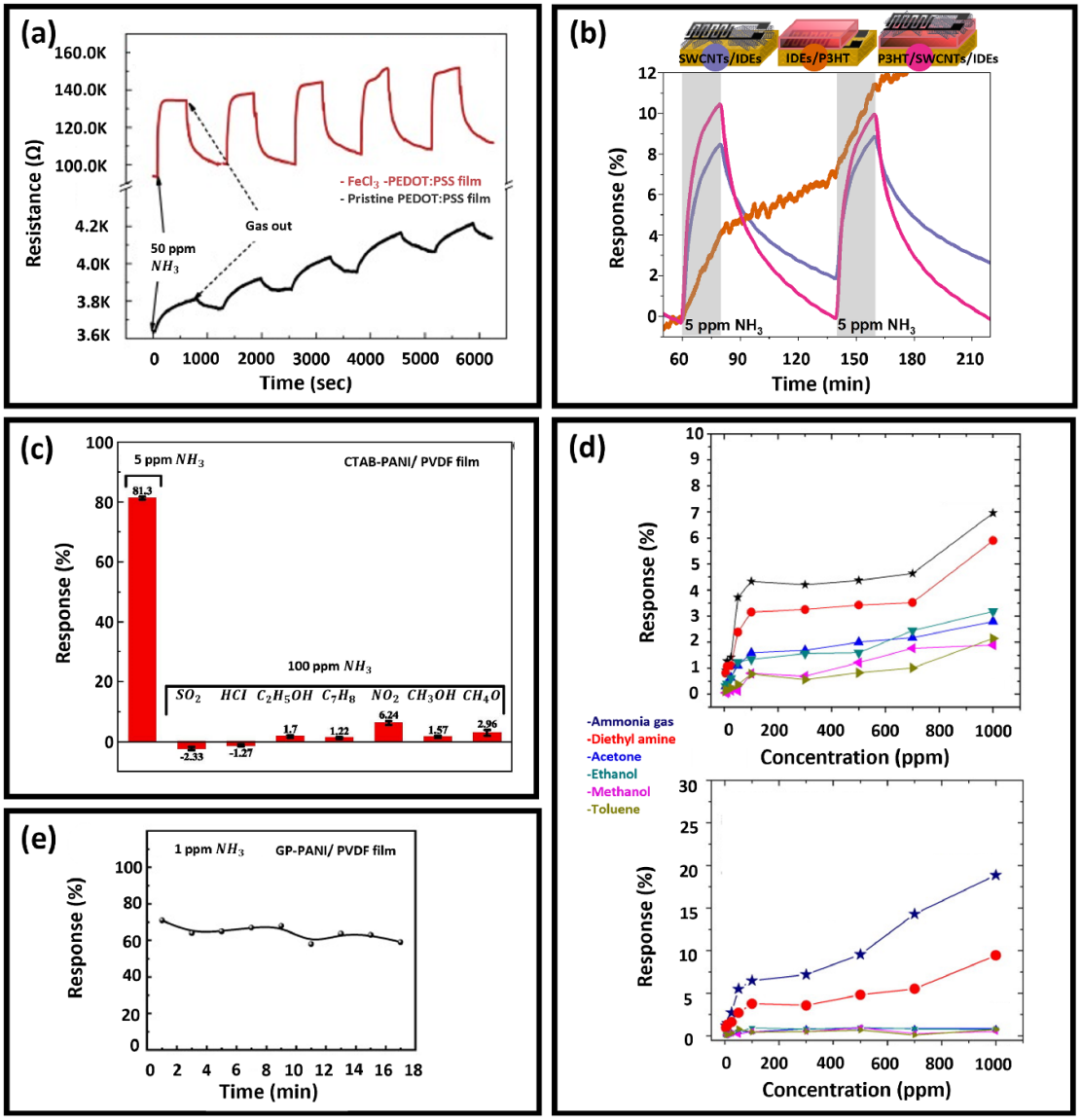

Figure 6. (a) Pristine PEDOT:PSS film and $FeCl_3$-PEDOT:PSS film resistance response towards 50 ppm NH_3. Reprinted from [98], Copyright (2019), with permission from Elsevier. (b) SWCNT, P3HT and P3HT/SWCNT sensor response exposed to 5 ppm of NH_3. Reproduced from [95], CC BY 4.0. (c) Selectivity of the CTAB-PANI/PVDF film. Reprinted from [107], Copyright (2023), with permission from Elsevier. (d) Gas responses of PEDOT:PSS (top) and graphene-PEDOT:PSS (bottom) gas sensors to various gases. Reprinted from [108], Copyright (2014), with permission from Elsevier. and (e) GP-PANI/PVDF film Long-term stability. Reprinted from [101], Copyright (2021), with permission from Elsevier.

obtained towards interfering gases such as 100 ppm H_2, C_3H_6O, C_2H_6O, CH_4O, C_7H_8, $CHCl_3$ while negative response values of between 0% and −4% were obtained for SO_2, CO, H_2S, and HCl. Instead, MWCNT-PANI/PVDF sensors developed by Wu *et al* [75] showed a response of 32% towards 1 ppm NH_3, while exposure towards 100 ppm of ethanol and acetone gave 3%, and towards methanol 2%. PANI/halloysite nanotubes (HNTs) sensors exposed to 10 ppm NH_3 gave a response value of ±90%, while the response value towards 10 ppm of other gases (H_2S, HCHO, CH_4, CO_2, CO, and SO_2), showed maximum obtained value of 12% for H_2S [74]. GP-PANI/PVDF showed response values below 5% towards 100 ppm CH_3OH, C_2H_6O, $(CH_2OH)_2$, C_3H_6O, and CH_2O and negative values staying between 0% and −3% for SO_2 and CO, while 1 ppm NH_3 results in a significantly larger response of 60% [101]. Hexadecyl trimethyl ammonium bromide (CTAB)-PANI/PVDF films gave a response of 81.3% for 5 ppm NH_3 while negative values for 100 ppm SO_2 and HCl between 0% and −3% were reached. Positive response values below 7% for C_2H_5OH, C_7H_8, NO_2, CH_3OH and CH_40 are depicted in figure 6(c) [107].

Compared to PANI based sensors, PEDOT:PSS devices show a lower sensitivity and selectivity. For instance, Seekaew *et al* [108] showed response values of 6.9% to NH_3, 5.9% to diethylamine, 3.2% to ethanol, 2.8% to acetone, 2.1% to toluene and 1.9% to methanol. However adding graphene to

Table 1. Conducting polymers (CPs) applied in chemiresistive sensors: addition, detection limit, response value, response time, recovery time, sensitivity, humidity, and substrate type.

Polymer	Addition	Detection limit	Response value	Response time	Recovery time	Sensitivity	Humidity	Substrate	References
PANI	no	<25 ppm	n.d.	n.d	> 50 min (50 ppm NH_3)	$y = 2.1053x + 80.387$ $R^2 = 0.9915$	5% RH	Si/SiO2	[127]
PANI	$SrGe_4O_9$	5.8% (250 ppt)	16% (0.2 ppm)	62 s (0.2 ppm)	223 s (0.2 ppm)	$y = 20.59x + 15.74$ $R^2 = 0.9900$	60 ± 5% RH	Polyimide (PI)	[99]
PANI	$Au@SiO_2$	1.6% (10 ppb)	± 80% (10 ppm)	35 s (10ppm)	133 s (10 ppm)	$y = 5.1x + 27.8$ $R^2 = 0.9879$	66% RH	Polyimide (PI)	[115]
PANI	MXene (Nb_2CT_x)	1.19% (20 ppb)	74.46% (10 ppm)	218 s (10 ppm)	300 s (10 ppm)	n.d.	87.1% RH	Polyimide (PI)	[100]
PANI	Graphene	10% (100 ppb)	60% (1 ppm)	46 s (1 ppm)	198 s (1 ppm)	n.d.	70% RH	Polyvinylidene fluoride (PVDF)	[101]
PANI	MWCNTs	8% (100 ppb)	32% (1 ppm)	76 s (1 ppm)	26 s (1 ppm)	$y = 20.91x + 8.12$ $R^2 = 0.93$	55 ± 3% RH	Polyvinylidene fluoride (PVDF)	[75]
PANI	PSS	9.4% (100 ppb)	70% (1 ppm)	160 s (1 ppm)	400 s (1 ppm)	$y = 8.862 + 64.328x R^2$ 0.998 89	65% RH	Polyvinylidene fluoride (PVDF)	[106]
PANI	$MCNTs/MoS_2$	11% (0.25 ppm)	40.12% (6 ppm)	32 s (0.25 ppm), 56 s (6 ppm)	36 s (0.25 ppm), 50 s (6 ppm)	$y = 22.41x^{0.34}$ R^2 0.9940	n.d.	FR4	[102]
PANI	Hexadecyl trimethyl ammonium bromide (CTAB)	3.5 ppb	4.6% (0.01ppm)	100 s	137 s	n.d.	40% RH	Polyvinylidene fluoride (PVDF)	[107]
PANI	Halloysite nanotubes (HNTs)	6.55% (10 ppb)	257.14% (50 ppm)	158 s (10 ppm)	162 s (10 ppm)	$y = 7.256\,19x + 20.161\,34$ ($R^2 - 0.993\,77$) $y = 3.9856x + 55.424$ ($R^2 = 0.992\,44$)	0%–90% RH	Polyimide (PI)	[74]

(Continued.)

Table 1. (Continued.)

PPy NPs	GO,RGO,SRGO	0.90 ppm, 0.035 ppm, 0.000 20 ppm	n.d.	81 s, 72 s, 48 s (1 ppm)	116 s, 151 s, 234 s (1 ppm)	Sensitivity 0.0033, 0.019, 4.06 (0.012)	Dry air	Fiber glass PCB	[128]
PPy	fiber/Ag with $LiClO_4$	0.25 ppm	1.46 (1 ppm)	$\leqslant$1 min (1 ppm)	$\leqslant$1 min (1 ppm)	$y = -8E{-}05x2 + 0.0445x + 1.2514$ R^2 0.9837	40% RH	Fiber glass PCB	[117]
PPy	SnO_2 nanofibers	57% (100 ppb)	1443% (50 ppm)	18 s (100 ppb), 44 s (50 ppm)	30 s (100 ppb), 62 s (50 ppm)	n.d.	50% RH	Alumina substrate (volt)	[103]
PPy	ZnO nanosheets	21% (500 ppb)	$\pm$76% (10 ppm)	256 s (5 ppm)	370 s (5 ppm)	n.d.	n.d.	Ceramic	[96]
PPyMPs	Silver nanoparticles (AgNPs)	0.12 ppm	n.d.	n.d.	n.d.	$y = 0.0161x + 0.0052$ ($R^2 = 0.9949$)	n.d.	Fiber glass PCB	[112]
PPy	MWCNT	5 ppm	17% (100 ppm)	47 s (100 ppm)	111 s (100 ppm)	$y = 0.14x + 2.5$ $R^2 = 0.988$	30 $\pm$ 2%	polyethylene terephthalate (PET)	[129]
PEDOT:PSS	ferric chloride ($FeCl_3$)	7.6% (500 ppb)	44% (50 ppm)	20 s (50 ppm)	n.d.	$y = 14.5x + 18.7$ R^2 0.962	60%–70%	polyimide (PI)	[98]
PEDOT:PSS	N-MXene ($Ti_3C_2T_x$)	2 ppm	13% (10 ppm)	280 s (10 ppm)	393.6 s (10 ppm)	5.6×10^{-3} /ppm R^2 0.995	36% RH (20, 36, 44, 53, 70% RH)	SiO2	[97]
PEDOT:PSS	f-MWCNT	66.3% (80 ppm)	66.3% (80 ppm)	$\pm$ 3.8 min	$\pm$4.5 min	0.97 ppm-1	dry-air	polyethylene terephthalate (PET)	[116]
PEDOT:PSS	Graphene	0.9% (5 ppm)	9.6% (500 ppm)	3 min	5 min	n.d.	56 $\pm$ 2% RH	flexible transparent	[108]
PEDOT:PSS	CuTSPc@3D-(N)GFs	10 ppm	18.7% (200 ppm)	138 s(200 ppm)	63 s (200 ppm)	n.d.	10 $\pm$ 2%RH	Si/SiO_2	[109]
P3HT	ZnO nanorods	1 ppm	25.1% (10 ppm)	0.9 s (1 ppm)	1.5 s (1 ppm)	$R^2 = 0.983$	Dry air	Si/SiO_2	[104]
P3HT	Au-loaded ZnO np	n.d.	32% (1000 ppm)	4.2 s (1000 ppm)	n.d.	n.d.	Dry air	Au/Al_2O_3	[113]
P3HT	SWCNTs	11.22% (5 ppm)	57.82% (50 ppm)	637 s (5 ppm)	$\leqslant$ 60 min	$y = 1.05^{*}x + 6.24$ $R^2 = 0.998\,88$	1.75 $\pm$ 1.40%RH	Polyimide (PI)	[95]

PEDOT:PSS increased the selectivity towards NH_3, the response towards NH_3 and diethylamine still shows similar response (of between 5%–7% for 1000 ppm NH_3) values as they contain similar amines functional groups (figure 6(d)). Instead, copper(II) tetrasulfophthalocyanine supported by a three-dimensional nitrogen-doped graphene framework (CuTSPc@3D-(N)GF)/PEDOT:PSS based sensors showed response values below 10% towards 200 ppm methanol, ethanol, acetone, toluene, chlorobenzene and water compared to a response of 18.7% towards 200 ppm NH_3 [109].

As these above cited examples show and the literature confirms [110], the use of only CPs is characterized by lower selectivity against several potential interfering gases. Meanwhile adding nanomaterials can significantly improve the selectivity. Even though it could be concluded from this section that good selectivity towards NH_3 can be achieved by selecting the right additions to the CPs, selectivity remains challenging, especially for gases that have a similar molecular structure compared to NH_3 such as diethylamine, as they both contain amine groups.

3.3. Stability of CP-based composites

Stability is defined as the capacity of a sensor to continue working under given conditions and to provide a steady performance over time giving the same output [111].

PANI based sensors show no big declines of the response values with less than 11% response value fluctuation according to the tested PANI sensors which are listed bellow. Stability of PANI/MWCNTs/MoS_2 was tested and showed no big variations for the following sensors when tested with concentrations of 1 ppm, 4 ppm and 20 ppm NH_3 over two months measured in intervals of 10 d [102]. PSS-PANI/PVDF films show that after one month the response value decreased from 70% to 65% [106]. MWCNT-PANI/PVDF showed stable response between 45% and 46% towards 2 ppm NH_3 over 22 d [75]. GP-PANI/PVDF was exposed to 1 ppm NH_3 for 17 d and showed a stable response value of ≈60% as indicated in figure 6(e) [101]. PANI/Nb_2CT_x showed less than 11% response value fluctuation within 35 d at high humidity of 87.1% [100].

For the other CPs only few sensors where tested for stability. PEDOT:PSS/N-MXene sensors showed a response disparity of 3.06% over 17 d [97]. An 8.2% decrease after 45 d towards 10 ppm NH_3 was observed for S-PPyMPs/AgNPs [112]. P3HT sensors stability was found to be reduced by 4.8% per day, while by addition of Au/ZnO nanoparticles (NPs) the reduction per day decreased and was 4.2% per day [113].

Thus, pristine CPs exhibit a reduction of their response over time, but good stability can be obtained with the right additions. For PANI the stability tests are reported in multiple papers, but for the other three (P3HT, PPy and PEDOT) only limit data is available.

3.4. Repeatability of CP-based composites

Repeatability is the ability of the sensor to produce identical responses when repeatably measured under the same specified conditions.

To test the precision of a sensor, repeatedly measurements with the same experimental conditions are used for a series of measurements in a short time interval to ideally produce identical response values [114]. Testing the repeatability of 20% Au@SiO_2 NCs doped PANI nanocomposites (NCs) doped PANI by exposing it to 3 × 10 ppm and 3 × 8 ppm showed a similar response as can be seen in figure 7(a) [115]. Polyaniline/$SrGe_4O_9$ was tested 4 times with 0.2 ppm NH_3 with response values of 18.1%, 16.8%, 16.0% and 15.7% [99]. Furthermore, good repeatability was found in all of the following sensors when exposed to: 4 × 80 ppm NH_3 (MWCNT-PEDOT:PSS) [116], 3 × 5 ppm NH_3 (PPy/ZnO) [96], 4 × 750 ppb (polypyrrole nanosphere/Ag) [117], 5 × 0.5 ppm, 1 ppm and 6 ppm (PANI/MWCNTs/MoS_2) [102], 5 × 1 ppm with less than 10% fluctuation (PSS-PANI/PVDF, MWCNT-PANI/PVDF and GP-PANI/PVDF) [75, 101, 106], 3 × 10 ppm NH_3 (PANI/Nb_2CT_x) [100], 5 × 5 ppm NH_3 (CTAB/PANI) [107], and 4 × 10 ppm NH_3 (PANI/HNTs) [74]. All of the above listed repeatability tests are only repeated for a maximum of six times, while Lawaniya *et al* [129] repeated the cycle for 15 times and exposed PPy-MWCNT sensors to 100 ppm NH_3.

To conclude on the stability of the devices, it could be argued whether less than 6 obtained cycles are a sufficient number to draw reliable conclusions on the stability.

3.5. Humidity interference of CP-based composites

CP gas sensors are often reported to be sensitive to water vapor [15]. Humidity is classified as absolute humidity and relative humidity [118]. Absolute humidity is the water vapor mass present in a specific volume of gas, while the relative humidity is the ratio of water vapor mass in a volume of gas to the maximum amount of water vapor the gas can contain at a specific temperature [119].

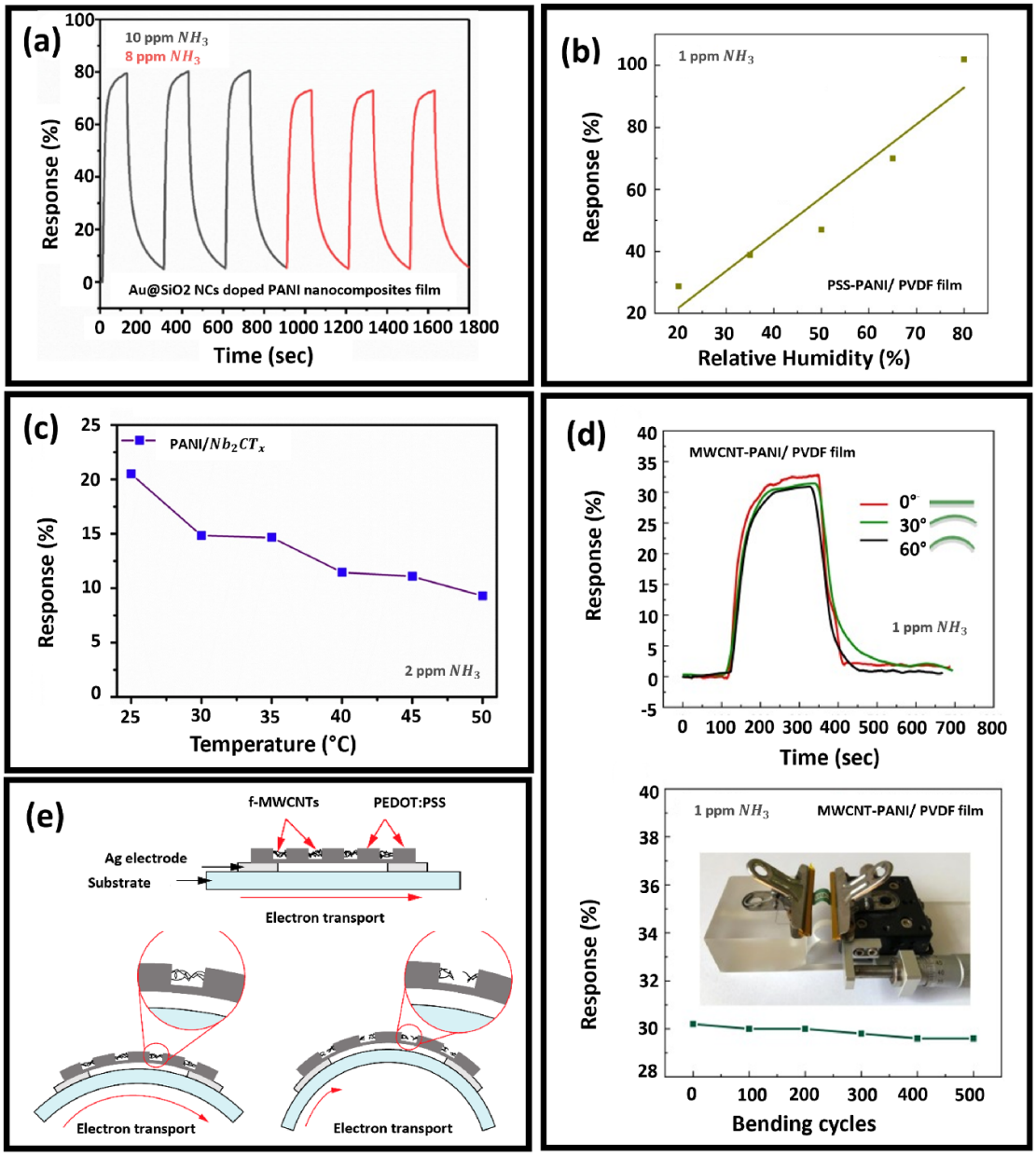

Figure 7. (a) Three repetition cycles at 10 ppm and 8 ppm NH_3 of 20% Au@SiO_2 NCs doped PANI nanocomposites films. Reprinted from [115], Copyright (2022), with permission from Elsevier. (b) Response of the PSS-PANI/PVDF film at different humidity levels. Reprinted from [106], Copyright (2021), with permission from Elsevier. (c) PANI/Nb_2CT_x sensors response values towards 2 ppm NH_3 in a temperature range from 25 °C–50 °C. Reprinted from [100], Copyright (2021), with permission from Elsevier. (d) MWCNT-PANI/PVDF film response-recovery curves towards 1 ppm NH_3 with bending angle of 0°, 30°, and 60° (top), and variation of the response value when exposed to 1 ppm NH_3 after between 0 and 500 bending cycles (bottom). Reprinted from [75], Copyright (2020), with permission from Elsevier (e) Schematic f-MWCNT-PEDOT:PSS electron transport during the flat state and for 3.0 cm and 0.9 cm bending radii. Reproduced from [116]. CC BY 4.0.

$FeCl_3$-PEDOT:PSS sensors showed an increase in response towards 50 ppm NH_3 with increasing humidity levels ranging of 25%–75% [98]. Qiu *et al* [97] reported the highest response value for 25 ppm NH_3 for PEDOT:PSS N-MXene sensors to be at 36% RH when testing humidity levels of 20%–70% RH. PPy/ZnO sensors show relatively low response values (0% to −20%) towards low and medium relative humidity values (10%–60% RH) while at high humidity values (60%–75% RH) the response values reach approximately −65% [96]. For PPy-MWCNT and PPy-SnO_2 sensors the response value reduces with an increase of the humidity levels ranging from 30% RH–90% RH [103, 129]. Beniwal and Sunny [103] noted a higher influence of humidity when exposed to higher ammonia concentrations of 100 ppm to 1000 ppm NH_3 compared to lower concentrations between 0.1 ppm and 10 ppm NH_3. When exposed to humidity levels ranging from 20%–80% RH, PANI sensors with additives of either PSS [106] (figure 7(b)), GP [101] or MWCNT [75] where exposed to 1 ppm NH_3 and showed increased response

values with an increase in humidity. Zhang *et al* [102] observed the same linear increase with humidity levels ranging from 11%–97% RH for PANI/MWCNTs/MoS_2. Similarly, Wang *et al* [100] found an improvement in response within the humidity range from 41% to 72.2% but a minor decline of 8.8% of the response values was found at high humidity levels of 72.2%–87.1% for PANI/Nb2CTx. Chen *et al* [115] found that the recovery time of Au@SiO_2 NCs/PANI sensors improved for sensing at 66% RH compared to 22% RH but also that the response values were higher at 22% RH.

Humidity can significantly influence NH_3 sensing, while the effect humidity has on CP gas sensors varies per sensor. Some sensors demonstrate an increased response with rising relative humidity levels [75, 96, 98, 101, 106], while others show reduced [103, 129] responses at higher humidity levels. This emphasizes the need to investigate the sensor response at specific humidity conditions to obtain accurate gas detection.

3.6. Temperature dependence of conductive polymer-based composites

Temperature variations cause variations in the electrical resistance of the gas sensing material [120]. Consequently, temperature fluctuations can changes in the sensor's output while the gas concentration remains constant [120]. Therefore it is of importance to determine the response of the CPs towards temperature.

The PANI/Nb_2CT_x composite shows a decrease of the response values to 2 ppm NH_3 when the temperature increases from 25 °C–50 °C (figure 7(c)) [100]. Additionally, PSS-PANI/PVDF sensors showed a decrease of their response value in a temperature range from 25 °C–50 °C when exposed to 1 ppm NH_3 [106]. Wu *et al* [75] found that MWCNT-PANI sensors exhibit an increase of resistance during an increase of temperature from 25 °C–50 °C.

PPy based sensors showed different behavior towards temperature depending on the additive. Kiani *et al* [117] found a gradual increase of the response values with increasing temperatures ranging from 22 °C till 70 °C in PPy sensors with additional Ag $LICIO_4$. At the same time, Lawaniya *et al* [129] observed a gradual decrease of the response value of PPy/MWCNT sensors when exposed to 100 ppm NH_3 within operating temperatures of 27 °C–100 °C. Dehsari *et al* [109] found that their PEDOT:PSS CuTSPc@3D-(N)GF sensors performed best at room temperature and show lower response values at increased temperatures when exposed to 200 ppm NH_3.

To conclude, temperature variations significantly influence the properties and response of gas sensing materials with varied behaviors observed for each CP. The response towards temperature may either increase or decrease depending on the additives.

3.7. Mechanical bendability of CP-based composites

Wearable gas sensor technologies are being developed for applications in medical diagnosis, food preservation, public safety, and environmental monitoring [121]. Wearable sensors with rigid substrates like glass or silicon wafers are inherently stiff, whereas mechanical flexibility is essential for them to conform comfortably to the body [121]. Flexible and stretchable substrates based on materials such as paper, polyimide (PI), polyethylene terephthalate (PET), polyethylene naphthalate (PEN), cotton and flexible glass, can overcome the limitations of rigid substrates [122, 123]. Flexible substrates allow the sensors to conform to various shapes [124]. The selection of the right CP for wearable gas sensors is of importance as for example PPy is mechanically rigid and brittle [125].

Recent advancements in substrate materials and fabrication techniques have further improved the mechanical properties of wearable gas sensors, with flexible porous polyvinylidene fluoride (PVDF) membranes being particularly promising due to their porous structure that enables gas permeability while maintaining mechanical strength [126]. The porous structure improves the air permeability of the sensors, making them more suitable for long-term wear without compromising gas detection performance [106]. Bending PVDF substrates which are covered with active MWCNT-PANI material to angles of 0°, 30°, and 60° resulted in a slight reduction of the response values (from 32% to 30.8% and 30.3%). 500 bending cycles to a 60° bending angle caused fluctuations of the response values of less than 10% as shown in figure 7(d) [75]. When PSS-PANI sensors fabricated on PVDF substrates where exposed to 2000 bending cycles to an bending angle of 120° the response value decreased from 70% to 60.8%. Here, the response value gradually stabilized between 3000–10000 bending cycles with response values of 57.2% to 54.9% for 1 ppm NH_3. Further testing the sensor for different bending angles of 120°, 180° and 240° resulted in a standard deviation of less than 10% [106]. GP-PANI/PVDF sensors were exposed to 1 ppm NH_3 as well as 0, 200, 500, 800, 1200 and 1500 bending cycles showed response values of 60%, 56%, 53%, 50%, 49% and 48%, respectively. It was observed that initially the resistances increased when the amount of bending cycles increased. After 1500 bending cycles the response value decreased from 60% to 48%, which gives a fluctuation within approximately 12%. This is a significant

improvement compared to pristine PANI sensors which reduced from 66% to 15% after 1500 bending cycles when exposed to 2 ppm NH_3 [101].

PANI Au@SiO_2 sensors fabricated on PI substrates were exposed to bending angles from −85° till 85° and kept a stable response value of 80% with a maximum concentration deviation of 0.6 ppm. Bending cycles (0, 50, 100, 150, 200, and 500 repetitions) with a bending angle of 60°, caused negligible variations of the response value [115]. PANI $SrGe_4O_9$ sensors on PI substrate showed a small error of the measured resistance value after 500 bending/extending cycles at an backward angle of 40° with an observed error of 0.25 ppm in measuring 2 ppm NH_3 [99]. The f-MWCNT-PEDOT:PSS sensors fabricated on PET were bent to curvature radii of 3.0 cm and 0.9 cm using polyactic acid (PLA) cylinders. Bending the sensor to a curvature radius of 3.0 cm resulted in a response between 67.5% and 65.0% while heavy substrate-bending to a 0.9 cm radius gave a response of 29.5%. After bending to 0.9 cm some cracks could be observed in the sensing film and a lack of MWCNT linkages bridging the crack gap on the sensing films was observed (the MWCNT act as connectors that promote electron transport), resulting in a low response towards NH_3, illustrated in figure 7(e) [116]. Bending of a PI substrate with sensors using $FeCl_3$-PEDOT:PSS as active material to angles of 120° (forward), 180° (flat), and 240° (backward) resulted in a standard deviation of the response value of less than 10% indicating good mechanical stability [98]. Bending graphene-PEDOT:PSS sensor on a flexible transparent substrate to angles ranging from 10° to 70° and exposure to 500 ppm NH_3 shows an increase of the response from 9.6% to 15.8% which corresponds to an increase of +6.2%. It is proposed that a polymer swelling process increases the inter-chain distance whereby NH_3 molecules can diffuse easily into the graphene polymer layer under bending induced strain [108].

Static bending to different angles, and also dynamic bending cycles can cause slight reductions of their response values [75, 101, 106], while some maintain a stable performance [115] even after hundreds of bending cycles.

4. Discussion

The performance of ammonia gas (NH_3) sensors depends heavily on the selection of the active sensing material. CPs present a promising option as active sensing layers due to their tunable chemical and physical properties, simplicity of fabrication, and cost-effectiveness. CPs such as polyaniline (PANI), polypyrrole (PPy), poly(3,4-ethylenedioxythiophene) (PEDOT), and poly(3-hexylthiophene) (P3HT) have already demonstrated significant effectiveness as sensing layers. Their electrical conductivity can be modulated through doping, making them versatile for various applications. The existing research on CPs underscores their potential for accurate and rapid NH_3 detection, especially with room-temperature operation.

Despite their advantages, CPs face challenges such as poor selectivity, reduced sensitivity, and environmental instability, including sensitivity to temperature and humidity. High humidity, for instance, can cause polymer swelling, altering conductivity and reducing sensitivity. Temperature fluctuations can further worsen performance instability. Reporting environmental factors like temperature and humidity during experiments is critical, as these parameters significantly affect sensor performance. Testing sensors across a range of NH_3 concentrations and under varied humidity levels can provide a comprehensive understanding of sensor capabilities.

A key challenge lies in comparing the performance of different CP-based NH_3 sensors due to the lack of standardized evaluation protocols. The absence of consistent protocols for determining sensitivity, response time, recovery time, and other key sensor parameters complicates the comparison of different sensors. To address this issue, establishing standardized experimental protocols for sensor performance characterization is crucial. A standardized approach will enable researchers to make meaningful comparisons and improve the overall performance of NH_3 sensors.

A proposed strategy for standardizing sensor testing includes measuring the sensor's resistance change at various NH_3 concentrations, such as baseline (0), 1, 3, 5, 10, 20, 25, 30, 40, 50, 75, and 100 ppm/ppb [54]. A minimum of five concentrations should be tested to generate a comprehensive response curve, including low, medium, and high concentrations to identify saturation points and define the full operational range. Testing with at least three sensor replicates is recommended to ensure reproducibility. It is also essential to report the temperature at which experiments are conducted, as temperature fluctuations, especially seasonal variations, can influence sensor performance. Humidity is another critical factor; it is advisable to characterize sensors under low, medium, and high humidity conditions (e.g. below 20%, 30%–60%, and above 90% RH, respectively) to assess its impact on sensor response. Additionally, for mechanical bendability experiments, both the bending radius and the strain induced by bending should be reported, as these factors depend on the substrate's properties and thickness.

Incorporating additives, creating nanostructured composites or nanoparticles, and introducing functional groups can improve the performance of CP-based sensors and can help address these limitations. These modifications can enhance selectivity, stability, and overall sensor performance.

Furthermore, selectivity is a key challenge, as gases with amine groups (e.g. diethylamine) share molecular similarities with NH_3 and can interfere with sensor detection. High selectivity toward NH_3 can be achieved by carefully selecting additives that enhance the specificity of the CP for NH_3 detection.

5. Future prospects

Future directions include increasing analyte diffusion into CP films by enhancing the surface area (increase porous structure, pore size and control film thickness) rather than using thick, continuous, amorphous, and bulky CP film matrices [130]. Adding to this, the chemical (e.g. charge transfer, hydrogen bonding, or redox reactions) and physical interactions (e.g. adsorption or surface-level interactions) between gases and CPs should be explored in greater detail using advanced theoretical modeling techniques [131]. Furthermore, more research on composite materials that improve performance (enhance electrical conductivity, improve selectivity, increase durability, increase flexibility) should be conducted to integrate them into the system. Nanoparticle aggregation can occur, so studying their distribution and adhesion methods is crucial [132]. Since CPs are relatively sensitive to moisture, temperature variations, and chemical degradation, materials that enhance stability should be extensively investigated [133, 134]. New CPs are synthesized regularly, and many less-explored CPs exist that can be tested for (NH_3) gas sensing capabilities. This creates an exciting future for advancements in NH_3 sensor technology [135, 136]. Finally, ensuring biocompatibility and low toxicity will be essential for safe use in medical or wearable applications.

6. Conclusion

CPs hold significant promise as active sensing layers in NH_3 gas sensors, offering versatility, cost-effectiveness, and the potential for room-temperature operation. Notably, CP-based NH_3 sensors, particularly those incorporating composite materials, have demonstrated success in detecting low concentrations of NH_3 with rapid response times, making them attractive for real-time monitoring in both biomedical and environmental applications. While these materials have demonstrated effectiveness, challenges such as selectivity, stability, and sensitivity to environmental conditions need to be addressed. Establishing standardized evaluation protocols is essential for meaningful sensor comparisons and overall technology improvement. By addressing these challenges and exploring new materials and methodologies, researchers can advance the development of high-performance NH_3 sensors for diverse applications.

Data availability statement

No new data were created or analysed in this study.

ORCID iDs

Annelot Nijkoops 0009-0007-9153-919X
Manuela Ciocca 0000-0001-8014-9814
Martina Aurora Costa Angeli 0000-0002-9302-4292
Mukhtar Ahmad 0000-0001-8514-2718
Remko Boom 0000-0003-2877-4166
Niko Münzenrieder 0000-0003-4653-5927
Paolo Lugli 0000-0002-2511-5643
Luisa Petti 0000-0003-0264-7185

References

[1] Shirakawa H 2001 The discovery of polyacetylene film - the dawning of an era of conducting polymers *Curr. Appl. Phys.* **1** 281–6
[2] Heeger A J 2007 Alan Graham MacDiarmid *Phys. Today* **60** 76–78
[3] Hangarter C M, Chartuprayoon N, Hernández S C, Choa Y and Myung N V 2013 Hybridized conducting polymer chemiresistive nano-sensors *Nano Today* **8** 39–55
[4] Tajik S, Beitollahi H, Nejad F G, Shoaie I S, Khalilzadeh M A, Asl M S, Van Le Q, Zhang K, Jang H W and Shokouhimehr M 2020 Recent developments in conducting polymers: applications for electrochemistry *RSC Adv.* **10** 37834–56
[5] Zeng Q, Cai P, Li Z, Qin J and Tang B Z 2008 An imidazole-functionalized polyacetylene: convenient synthesis and selective chemosensor for metal ions and cyanide *Chem. Commun.* 1094

[6] Su M-j, Wan W, Yong X, Lu X-w, Liu R-y and Qu J-q 2013 Urea-based polyacetylenes as an optical sensor for fluoride ions *Chin. J. Polym. Sci.* **31** 620–9
[7] Li Y and Yang M J 2002 Humidity sensitive properties of substituted polyacetylenes *Synth. Met.* **129** 285–90
[8] Li Y and Yang M J 2002 Bilayer thin film humidity sensors based on sodium polystyrenesulfonate and substituted polyacetylenes *Sensors Actuators B* **87** 184–9
[9] Shirakawa H, McDiarmid A and Heeger A 2003 Focus article: twenty-five years of conducting polymers *Chem. Commun.* 1–4
[10] Bhandari S 2017 *Polyaniline: Structure and Properties Relationship* (Elsevier Inc.) http://dx.doi.org/10.1016/B978-0-12-809551-5.00002-3
[11] Das T K and Prusty S 2012 Review on conducting polymers and their applications *Polym.-Plast. Technol. Eng.* **51** 1487–500
[12] Salehi A, Naderi P, Boroumand F A and Dunbar A, Fabrication and characterization of hybrid photovoltaic devices based on N-type GaAs and polymer composites 2018 (https://doi.org/10.11159/ehst18.116)
[13] Liu X, Zheng W, Kumar R, Kumar M and Zhang J 2022 Conducting polymer-based nanostructures for gas sensors *Coord. Chem. Rev.* **462** 214517
[14] Wang Y, Liu A, Han Y and Li T 2020 Sensors based on conductive polymers and their composites: a review *Polym. Int.* **69** 7–17
[15] Bai H and Shi G 2007 Gas sensors based on conducting polymers *Sensors* **7** 267–307
[16] Namsheer K and Rout C S 2021 Conducting polymers: a comprehensive review on recent advances in synthesis, properties and applications *RSC Adv.* **11** 5659–97
[17] Yan Y, Yang G, Xu J-L, Zhang M, Kuo C-C and Wang S-D 2020 Conducting polymer-inorganic nanocomposite-based gas sensors: a review *Sci. Technol. Adv. Mater.* **21** 768–86
[18] Behera S N, Sharma M, Aneja V P and Balasubramanian R 2013 Ammonia in the atmosphere: a review on emission sources, atmospheric chemistry and deposition on terrestrial bodies *Environ. Sci. Pollut. Res.* **20** 8092–131
[19] Warner J X, Dickerson R R, Wei Z, Strow L L, Wang Y and Liang Q 2017 Increased atmospheric ammonia over the world's major agricultural areas detected from space *Geophys. Res. Lett.* **44** 2875–84
[20] Timmer B, Olthuis W and v. d. Berg A 2005 Ammonia sensors and their applications-a review *Sensors Actuators B* **107** 666–77
[21] Thomsen K L, Eriksen P L, Kerbert A J, De Chiara F, Jalan R and Vilstrup H 2023 Role of ammonia in NAFLD: an unusual suspect *JHEP Reports* **5** 100780
[22] Kurmi K and Haigis M C 2020 Nitrogen metabolism in cancer and immunity *Trends Cell Biol.* **30** 408–24
[23] Nijkoops A, Ciocca M, Angeli M A C, Pogliaghi S, Krik S, Avancini E, Münzenrieder N, Lugli P and Petti L 2025 Ammonia dynamics in the human body: insights in biomedical sensing technologies *Adv. Sensor Res.* **4** 2400179
[24] Hibbard T and Killard A J 2011 Breath ammonia analysis: clinical application and measurement *Crit. Rev. Anal. Chem.* **41** 21–35
[25] Dhall S, Mehta B R, Tyagi A K and Sood K 2021 A review on environmental gas sensors: materials and technologies *Sensors Int.* **2** 100116
[26] Lee D D 2001 Environmental gas sensors *IEEE Sens. J.* **1** 214–24
[27] Di Natale C, Paolesse R, Martinelli E and Capuano R 2014 Solid-state gas sensors for breath analysis: a review *Anal. Chim. Acta* **824** 1–17
[28] Okechukwu V O, Idris A O, Umukoro E H, Azizi S and Maaza M 2024 Exploring the contribution of intelligent nanomaterials in gas sensing *ChemistrySelect* **9** e202304703
[29] Hodgkinson J and Tatam R P 2013 Optical gas sensing: a review *Meas. Sci. Technol.* **24** 012004
[30] Khaled A Y, Aziz S A, Bejo S K, Nawi N M, Seman I A and Onwude D I 2018 Early detection of diseases in plant tissue using spectroscopy applications and limitations *Appl. Spectrosc. Rev.* **53** 36–64
[31] Elsherif M *et al* 2022 Optical Fiber Sensors: working Principle, Applications and Limitations *Adv. Photon. Res.* **3** 11
[32] Khan M A, Qazi F, Hussain Z, Idrees M U, Soomro S and Soomro S 2017 Recent trends in electrochemical detection of NH3, H2S and NOx gases *Int. J. Electrochem. Sci.* **12** 1711–33
[33] Zhang W, Wang R, Luo F, Wang P and Lin Z 2020 Miniaturized electrochemical sensors and their point-of-care applications *Chin. Chem. Lett.* **31** 589–600
[34] Raninec M Overcoming the technical challenges of electrochemical gas sensing *Technical Report* (available at: https://www.analog.com/en/resources/technical-articles/overcoming-the-technical-challenges-of-electrochemical-gas-sensing.html)
[35] Reddy B K S and Borse P H 2021 Review-recent material advances and their mechanistic approaches for room temperature chemiresistive gas sensors *J. Electrochem. Soc.* **168** 057521
[36] Barhoum A, Hamimed S, Slimi H, Othmani A, Abdel-Haleem F M and Bechelany M 2023 Modern designs of electrochemical sensor platforms for environmental analyses: principles, nanofabrication opportunities and challenges *Trends Environ. Anal. Chem.* **38** e00199
[37] Srinivasan P, Ezhilan M, Kulandaisamy A J, Babu K J and Rayappan J B B 2019 Room temperature chemiresistive gas sensors: challenges and strategies-a mini review *J. Mater. Sci., Mater. Electron.* **30** 15825–47
[38] Nasiri N and Clarke C 2019 Nanostructured chemiresistive gas sensors for medical applications *Sensors* **19** 462
[39] Liu X, Cheng S, Liu H, Hu S, Zhang D and Ning H 2012 A survey on gas sensing technology *Sensors* **12** 9635–65
[40] Korotcenkov G 2007 Metal oxides for solid-state gas sensors: what determines our choice? *Mater. Sci. Eng. B* **139** 1–23
[41] Yang S, Jiang C and Wei S-H 2017 Gas sensing in 2D materials *Appl. Phys. Rev.* **4** 021304
[42] Lugli P *et al* 2023 Solution-processable carbon nanotubes for sensing and biosensing applications *2023 IEEE Nanotechnology Materials and Devices Conf. (NMDC)* (IEEE) pp 655–9
[43] Dey A 2018 Semiconductor metal oxide gas sensors: a review *Mater. Sci. Eng. B* **229** 206–17
[44] Ahmed S and Sinha S K 2022 Studies on nanomaterial-based p-type semiconductor gas sensors *Environ. Sci. Pollut. Res.* **30** 24975–86
[45] Saruhan B, Fomekong R L and Nahirniak S 2021 Review: influences of semiconductor metal oxide properties on gas sensing characteristics *Front. Sens.* **2** 1–24
[46] Saleemi M A, Fouladi M H, Yong P V C, Chinna K, Palanisamy N K and Wong E H 2021 Toxicity of carbon nanotubes: molecular mechanisms, signaling cascades and remedies in biomedical applications *Chem. Res. Toxicol.* **34** 24–46
[47] Baharuddin A A, Ang B C, Haseeb A, Wong Y C and Wong Y H 2019 Advances in chemiresistive sensors for acetone gas detection *Mater. Sci. Semicond. Process.* **103** 104616
[48] Naganaboina V R, Bonam S, Anandkumar M, Deshpande A S and Singh S G 2023 Improved chemiresistor gas sensing response by optimizing the applied electric field and interdigitated electrode geometry *Mater. Chem. Phys.* **305** 127975
[49] Wong Y C, Ang B C, Haseeb A S M A, Baharuddin A A and Wong Y H 2020 Review-conducting polymers as chemiresistive gas sensing materials: a review *J. Electrochem. Soc.* **167** 037503

[50] Fu L, You S, Li G, Li X and Fan Z 2023 Application of semiconductor metal oxide in chemiresistive methane gas sensor: recent developments and future perspectives *Molecules* **28** 6710
[51] Jian Y, Hu W, Zhao Z, Cheng P, Haick H, Yao M and Wu W 2020 Gas sensors based on chemi-resistive hybrid functional nanomaterials *Nano-Micro Lett.* **12** 71
[52] Majhi S M, Mirzaei A, Kim H W, Kim S S and Kim T W 2021 Recent advances in energy-saving chemiresistive gas sensors: a review *Nano Energy* **79** 105369
[53] Fàbrega C, Casals O, Hernández-Ramírez F and Prades J D 2018 A review on efficient self-heating in nanowire sensors: prospects for very-low power devices *Sens. Actuators B* **256** 797–811
[54] Kwak D, Lei Y and Maric R 2019 Ammonia gas sensors: a comprehensive review *Talanta* **204** 713–30
[55] Rigoni F, Tognolini S, Borghetti P, Drera G, Pagliara S, Goldoni A and Sangaletti L 2014 Environmental monitoring of Low-PPB ammonia concentrations based on single-wall carbon nanotube chemiresistor gas sensors: detection limits, response dynamics and moisture effects *Proc. Eng.* **87** 716–9
[56] Huang Y, Wieck L and Tao S 2013 Development and evaluation of optical fiber NH3 sensors for application in air quality monitoring *Atmos. Environ.* **66** 1–7
[57] Javed U, Ramaiyan K P, Kreller C R, Brosha E L, Mukundan R and Morozov A V 2018 Using sensor arrays to decode NO /NH3/C3H8 gas mixtures for automotive exhaust monitoring *Sens. Actuators B* **264** 110–8
[58] Li H-Y, Lee C-S, Kim D H and Lee J-H 2018 Flexible room-temperature NH_3 sensor for ultrasensitive, selective and humidity-independent gas detection *ACS Appl. Mater. Interfaces* **10** 27858–67
[59] Meng F J, Xin R F and Li S X 2023 Metal oxide heterostructures for improving gas sensing properties: a review *Materials* **16** 263
[60] Le T-H, Kim Y and Yoon H 2017 Electrical and electrochemical properties of conducting polymers *Polymers* **9** 150
[61] Bredas J L and Street G B 1985 Polarons, bipolarons and solitons in conducting polymers *Acc. Chem. Res.* **18** 309–15
[62] Park Y, Jung J and Chang M 2019 Research progress on conducting polymer-based biomedical applications *Appl. Sci.* **9** 1070
[63] Wu X, Fu W and Chen H 2022 Conductive polymers for flexible and stretchable organic optoelectronic applications *ACS Appl. Polym. Mater.* **4** 4609–23
[64] Chauhan M, Bhardwaj S K, Bhanjana G, Kumar R, Dilbaghi N, Kumar S and Chaudhary G R 2019 Conducting Polymers and Metal-Organic Frameworks as Advanced Materials for Development of Nanosensors *Advances in Nanosensors for Biological and Environmental Analysis* (Elsevier) pp 43–62
[65] Wang Y, Jia W, Strout T, Schempf A, Zhang H, Li B, Cui J and Lei Y 2009 Ammonia gas sensor using polypyrrole-coated TiO 2 /ZnO nanofibers *Electroanalysis* **21** 1432–8
[66] Arafat M M, Dinan B, Akbar S A and Haseeb A S M A 2012 Gas sensors based on one dimensional nanostructured metal-oxides: a review *Sensors* **12** 7207–58
[67] Sengupta P P, Barik S and Adhikari B 2006 Polyaniline as a gas-sensor material *Mater. Manuf. Process.* **21** 263–70
[68] Zhang R, Wang Y, Li J, Zhao H, Wang Y and Zhou Y 2022 Mesoporous cellulose nanofibers-interlaced PEDOT:PSS hybrids for chemiresistive ammonia detection *Microchim. Acta* **189** 308
[69] Bhat N V, Gadre A P and Bambole V A 2001 Structural, mechanical, and electrical properties of electropolymerized polypyrrole composite films *J. Appl. Polym. Sci.* **80** 2511–7
[70] Malhotra B, Dhand C, Lakshminarayanan R, Dwivedi N, Mishra S, Solanki P, Venkatesh M, Beuerman R W and Ramakrishna S 2015 Polyaniline-based biosensors *Nanobiosensors Dis. Diagn.* **4** 25
[71] Korent A, Trafela x016E;, Soderžnik K x016E;, Samardžija Z, Šturm S and Rožman K x016E; 2022 Au-decorated electrochemically synthesised polyaniline-based sensory platform for amperometric detection of aqueous ammonia in biological fluids *Electrochim. Acta* **430** 141034
[72] Wang S, Liu B, Duan Z, Zhao Q, Zhang Y, Xie G, Jiang Y, Li S and Tai H 2021 PANI nanofibers-supported Nb2CTx nanosheets-enabled selective NH3 detection driven by TENG at room temperature *Sens. Actuators B* **327** 128923
[73] Nakate U T, Choudhury S P, Ahmad R, Patil P, Nakate Y T and Hahn Y B 2020 *Functional Nanomaterials* (*Materials Horizons: From Nature to Nanomaterials*), ed S Thomas, N Joshi and V K Tomer (Springer) (https://doi.org/10.1007/978-981-15-4810-9)
[74] Duan X, Duan Z, Zhang Y, Liu B, Li X, Zhao Q, Yuan Z, Jiang Y and Tai H 2022 Enhanced NH3 sensing performance of polyaniline via a facile morphology modification strategy *Sens. Actuators B* **369** 132302
[75] Wu T, Lv D, Shen W, Song W and Tan R 2020 Trace-level ammonia detection at room temperature based on porous flexible polyaniline/polyvinylidene fluoride sensing film with carbon nanotube additives *Sens. Actuators B* **316** 128198
[76] Scharber M C and Sariciftci N S 2021 Low band gap conjugated semiconducting polymers *Adv. Mater. Technol.* **6** 2000857
[77] Abdelhamid M E, O'Mullane A P and Snook G A 2015 Storing energy in plastics: a review on conducting polymers & their role in electrochemical energy storage *RSC Adv.* **5** 11611–26
[78] Anand D and Khandelwal M 2015 Conducting flexible paper based on Bacterial cellulose and Polyaniline composites *PhD Dissertation* Indian Institute of Technology Hyderabad (https://doi.org/10.13140/RG.2.1.3321.1764)
[79] Coropceanu V, Cornil J, da Silva Filho D A, Olivier Y, Silbey R and Brédas J L 2007 Charge transport in organic semiconductors *Chem. Rev.* **107** 926–52
[80] Cheng Y J, Yang S H and Hsu C S 2009 Synthesis of conjugated polymers for organic solar cell applications *Chem. Rev.* **109** 5868–923
[81] Castagnola V 2015 Implantable microelectrodes on soft substrate with nanostructured active surface for stimulation and recording of brain activities (available at: https://theses.hal.science/tel-01137352/)
[82] Xin H, Subramaniyan S, Kwon T-W, Shoaee S, Durrant J R and Jenekhe S A 2012 Enhanced open circuit voltage and efficiency of donor-acceptor copolymer solar cells by using Indene-C60 Bisadduct *Chem. Mater.* **24** 1995–2001
[83] Perumal A, Faber H, Yaacobi-Gross N, Pattanasattayavong P, Burgess C, Jha S, McLachlan M A, Stavrinou P N, Anthopoulos T D and Bradley D D C 2015 High-efficiency, solution-processed, multilayer phosphorescent organic light-emitting diodes with a copper thiocyanate hole-injection/hole-transport layer *Adv. Mater.* **27** 93–100
[84] Xiao Y, Han G, Chang Y, Zhou H, Li M and Li Y 2014 An all-solid-state perovskite-sensitized solar cell based on the dual function polyaniline as the sensitizer and p-type hole-transporting material *J. Power Sources* **267** 1–8, 12
[85] Anjaneyulu P, Varade V, Sangeeth C S S, Ramesh K P and Menon R 2014 Field dependent and disorder-induced nonlinear charge transport in electrochemically doped polypyrrole devices *J. Phys. D: Appl. Phys.* **47** 505106
[86] Zhu T *et al* 2023 Formation of hierarchically ordered structures in conductive polymers to enhance the performances of lithium-ion batteries *Nat. Energy* **8** 129–37
[87] Xu Y, Wang X and Hao Q 2021 A mini review on thermally conductive polymers and polymer-based composites *Compos. Commun.* **24** 100617

[88] Lim J A, Liu F, Ferdous S, Muthukumar M and Briseno A L 2010 Polymer semiconductor crystals *Mater. Today* **13** 14–24
[89] Kim N-J, Kwon J-H and Kim M 2013 Highly oriented self-assembly of conducting polymer chains: extended-chain crystallization during long-range polymerization *J. Phys. Chem. C* **117** 15402–8
[90] Xu X, Zhou J and Chen J 2020 Thermal transport in conductive polymer-based materials *Adv. Funct. Mater.* **30** 1–18
[91] Shi W, Yildirim E, Wu G, Wong Z M, Deng T, Wang J, Xu J and Yang S 2020 The role of electrostatic interaction between free charge carriers and counterions in thermoelectric power factor of conducting polymers: from crystalline to polycrystalline domains *Adv. Theory Simul.* **3** 1–10
[92] Brinkmann M, Hartmann L, Biniek L, Tremel K and Kayunkid N 2014 Orienting semi-conducting π-conjugated polymers *Macromol. Rapid Commun.* **35** 9–26
[93] Magurudeniya H D, Huang P, Gunathilake S S, Rainbolt E A, Biewer M C and Stefan M C 2014 Semiconducting polymers: poly(thiophenes) *Encyclopedia Polym. Sci. Technol.* 1–36
[94] Xiao L L, Zhou X, Yue K and Guo Z H 2021 Synthesis and self-assembly of conjugated block copolymers *Polymers* **13** 1–20
[95] Nijkoops A, Ciocca M, Krik S, Douaki A, Gurusekaran A, Vasquez S, Petrelli M, Angeli M A C, Petti L and Lugli P 2023 Flexible and printed chemiresistive ammonia gas sensors based on carbon nanotube and conjugated polymers: a comparison of response and recovery performance *IEEE Sens. Lett.* **7** 1–4
[96] Li Y, Jiao M and Yang M 2017 *In − situ* grown nanostructured ZnO via a green approach and gas sensing properties of polypyrrole/ZnO nanohybrids *Sens. Actuators B* **238** 596–604
[97] Qiu J, Xia X, Hu Z, Zhou S, Wang Y, Wang Y, Zhang R, Li J and Zhou Y 2021 Molecular ammonia sensing of PEDOT:PSS/nitrogen doped MXene Ti3C2Txcomposite film at room temperature *Nanotechnology* **33** 065501
[98] Lv D, Chen W, Shen W, Peng M, Zhang X, Wang R, Xu L, Xu W, Song W and Tan R 2019 Enhanced flexible room temperature ammonia sensor based on PEDOT: PSS thin film with FeCl3 additives prepared by inkjet printing *Sens. Actuators B* **298** 126890
[99] Zhang Y, Zhang J, Jiang Y, Duan Z, Liu B, Zhao Q, Wang S, Yuan Z and Tai H 2020 Ultrasensitive flexible NH3 gas sensor based on polyaniline/SrGe4O9 nanocomposite with PPT-level detection ability at room temperature *Sens. Actuators B* **319** 128293
[100] Wang S, Jiang Y, Liu B, Duan Z, Pan H, Yuan Z, Xie G, Wang J, Fang Z and Tai H 2021 Ultrathin Nb2CT nanosheets-supported polyaniline nanocomposite: enabling ultrasensitive NH3 detection *Sens. Actuators B* **343** 130069
[101] Wu Q, Shen W, Lv D, Chen W, Song W and Tan R 2021 An enhanced flexible room temperature ammonia gas sensor based on GP-PANI/PVDF multi-hierarchical nanocomposite film *Sens. Actuators B* **334** 129630
[102] Zhang D, Wu Z, Li P, Zong X, Dong G and Zhang Y 2018 Facile fabrication of polyaniline/multi-walled carbon nanotubes/molybdenum disulfide ternary nanocomposite and its high-performance ammonia-sensing at room temperature *Sens. Actuators B* **258** 895–905
[103] Beniwal A and Sunny 2019 Electrospun SnO2/PPy nanocomposite for ultra-low ammonia concentration detection at room temperature *Sens. Actuators B* **296** 126660
[104] Han K-X, Wu C-C, Hsu W-F, Chien W and Yang C-F 2023 Preparation of ultrafast ammonia sensor based on cross-linked ZnO nanorods coated with poly(3-hexylthiophene) *Synth. Met.* **299** 117449
[105] Feng S, Farha F, Li Q, Wan Y, Xu Y, Zhang T and Ning H 2019 Review on smart gas sensing technology *Sens.* **19** 3760
[106] Lv D, Shen W, Chen W, Tan R, Xu L and Song W 2021 PSS-PANI/PVDF composite based flexible NH3 sensors with sub-ppm detection at room temperature *Sens. Actuators B* **328** 129085
[107] Zhao J, Shen W, Lv D, Zhang J, Wang Y, Liang T and Song W 2023 Flexible room temperature sensor with modulation of polyaniline interfacial polymerization by CTAB for ppb-level ammonia detection *Mater. Lett.* **333** 133690
[108] Seekaew Y, Lokavee S, Phokharatkul D, Wisitsoraat A, Kerdcharoen T and Wongchoosuk C 2014 Low-cost and flexible printed graphene-PEDOT:PSS gas sensor for ammonia detection *Org. Electron.* **15** 2971–81
[109] Dehsari H S, Gavgani J N, Hasani A, Mahyari M, Shalamzari E K, Salehi A and Taromi F A 2015 Copper(ii) phthalocyanine supported on a three-dimensional nitrogen-doped graphene/PEDOT-PSS nanocomposite as a highly selective and sensitive sensor for ammonia detection at room temperature *RSC Adv.* **5** 79729–37
[110] Sudheep C, Verma A, Jasrotia P, Hmar J J L, Gupta R, Verma A S, Jyoti A K and Kumar T 2024 Revolutionizing gas sensors: the role of composite materials with conducting polymers and transition metal oxides *Res. Chem.* **7** 101255
[111] Kalantar-zadeh K 2013 *Sensors: An Introductory Course* vol 9781461450 (Springer) (https://doi.org/10.1007/978-1-4614-5052-8)
[112] Kamalabadi M, Ghoorchian A, Derakhshandeh K, Gholyaf M and Ravan M 2022 Design and fabrication of a gas sensor based on a polypyrrole/silver nanoparticle film for the detection of ammonia in exhaled breath of COVID-19 patients suffering from acute kidney injury *Anal. Chem.* **94** 16290–8
[113] Kruefu V, Wisitsoraat A, Tuantranont A and Phanichphant S 2014 Gas sensing properties of conducting polymer/Au-loaded ZnO nanoparticle composite materials at room temperature *Nanoscale Res. Lett.* **9** 467
[114] Chiavaioli F, Gouveia C, Jorge P and Baldini F 2017 Towards a uniform metrological assessment of grating-based optical fiber sensors: from refractometers to biosensors *Biosensors* **7** 23
[115] Chen G, Yuan Y, Lang M, Lv Z, Ma W, Gu N, Liu H, Fang J, Zhang H and Cheng Y 2022 Core-shell Au@SiO2 nanocrystals doped PANI for highly sensitive, reproducible and flexible ammonia sensor at room temperature *Appl. Surf. Sci.* **598** 153821
[116] Boonthum D, Oopathump C, Fuengfung S, Phunudom P, Thaibunnak A, Juntong N, Rungruang S and Pakdee U 2022 Screen-printing of functionalized MWCNT-PEDOT:PSS based solutions on bendable substrate for ammonia gas sensing *Micromachines* **13** 462
[117] Kiani G, Nourizad A and Nosrati R 2018 *In − situ* chemical synthesis of polypyrrole/silver nanocomposite for the use as a room temperature ammonia gas sensor *Fibers Polym.* **19** 2188–94
[118] Lee C-Y and Lee G-B 2005 Humidity sensors: a review *Sens. Lett.* **3** 1–15
[119] Green J and Dyer I 2009 Measurement of humidity *Anaesthesia Intensive Care Med.* **10** 45–47
[120] Megha R, Ali F A, Ravikiran Y, Ramana C, Kumar A K, Mishra D, Vijayakumari S and Kim D 2018 Conducting polymer nanocomposite based temperature sensors: a review *Inorg. Chem. Commun.* **98** 11–28
[121] Lawaniya S D, Kumar S, Yu Y, Rubahn H-G, Mishra Y K and Awasthi K 2023 Functional nanomaterials in flexible gas sensors: recent progress and future prospects *Mater. Today Chem.* **29** 101428
[122] Costa J C, Spina F, Lugoda P, Garcia-Garcia L, Roggen D and Münzenrieder N 2019 Flexible sensors-from materials to applications *Technologies* **7** 35
[123] Luo Y *et al* 2023 Technology roadmap for flexible sensors *ACS Nano* **17** 5211–95
[124] Pecunia V *et al* 2024 Roadmap on printable electronic materials for next-generation sensors *Nano Futures* **8** 032001
[125] Kaur G, Adhikari R, Cass P, Bown M and Gunatillake P 2015 Electrically conductive polymers and composites for biomedical applications *RSC Adv.* **5** 37553–67

[126] Dallaev R, Pisarenko T, Sobola D, Orudzhev F, Ramazanov S and Trčka T 2022 Brief review of PVDF properties and applications potential *Polymers* **14** 4793
[127] Le D D, Nguyen T N N, Doan D C T, Dang T M D and Dang M C 2016 Fabrication of interdigitated electrodes by inkjet printing technology for apllication in ammonia sensing *Adv. Nat. Sci.: Nanosci. Nanotechnol.* **7** 025002
[128] Shahmoradi A, Hosseini A, Akbarinejad A and Alizadeh N 2021 Noninvasive detection of ammonia in the breath of hemodialysis patients using a highly sensitive ammonia sensor based on a polypyrrole/sulfonated graphene nanocomposite *Anal. Chem.* **93** 6706–14
[129] Lawaniya S D, Meena N, Kumar S, Yu Y-T and Awasthi K 2023 Effect of MWCNTs Incorporation Into Polypyrrole (PPy) on ammonia sensing at room temperature *IEEE Sens. J.* **23** 1837–44
[130] Tran V V, Jeong G, Kim K S, Kim J, Jung H R, Park B, Park J J and Chang M 2022 Facile strategy for modulating the nanoporous structure of ultrathin π-conjugated polymer films for high-performance gas sensors *ACS Sensors* **7** 175–85
[131] Liu Y, Gao S, Zhang X, Xin J H and Zhang C 2022 Probing the nature of charge carriers in one-dimensional conjugated polymers: a review of the theoretical models, experimental trends and thermoelectric applications *J. Mater. Chem.* **11** 12–47
[132] Verma A, Gupta R, Verma A S and Kumar T 2023 A review of composite conducting polymer-based sensors for detection of industrial waste gases *Sens. Actuators Rep.* **5** 100143
[133] Aly K I, Younis O, Mahross M H, Orabi E A, Abdel-Hakim M, Tsutsumi O, Mohamed M G and Sayed M M 2019 Conducting copolymers nanocomposite coatings with aggregation-controlled luminescence and efficient corrosion inhibition properties *Prog. Organic Coatings* **135** 525–35
[134] g. Lee J, Cho W, Kim Y, Cho H, Lee H and Kim J H 2019 Formation of a conductive overcoating layer based on hybrid composites to improve the stability of flexible transparent conductive films *RSC Adv.* **9** 4428–34
[135] Prunet G, Pawula F, Fleury G, Cloutet E, Robinson A J, Hadziioannou G and Pakdel A 2021 A review on conductive polymers and their hybrids for flexible and wearable thermoelectric applications *Mater. Today Phys.* **18** 100402
[136] Le C V and Yoon H 2024 Advances in the use of conducting polymers for healthcare monitoring *Int. J. Mol. Sci.* **25** 1564